Mon. Not. R. Astron. Soc. **334,** 553–562 (2002)

X-rays from isolated black holes in the Milky Way

Eric Agol★† and Marc Kamionkowski
California Institute of Technology, Mail Code 130-33, Pasadena, CA 91125, USA

Accepted 2002 March 22. Received 2002 February 22; in original form 2001 October 2

ABSTRACT

Galactic stellar-population-synthesis models, chemical-enrichment models, and possibly gravitational microlensing indicate that about $N_{\rm tot} = 10^8 - 10^9$ stellar-mass black holes reside in our Galaxy. We study X-ray emission from accretion from the interstellar medium on to isolated black holes. Although black holes may be fewer in number than neutron stars, $N_{\rm NS} \sim 10^9$, their higher masses, $\langle M \rangle \sim 9\,{\rm M}_\odot$, and smaller space velocities, $\sigma_v \sim 40\,{\rm km\,s^{-1}}$, result in Bondi–Hoyle accretion rates $\sim 4 \times 10^3$ times higher than for neutron stars. Given a total number of black holes $N_{\rm tot} = N_9 10^9$ within the Milky Way, we estimate that $\sim 10^3 N_9$ should accrete at $\dot{M} > 10^{15}\,{\rm g\,s^{-1}}$, comparable to accretion rates inferred for black hole X-ray binaries. If black holes accrete at the Bondi–Hoyle rate with efficiencies only $\sim 10^{-4}(N_{\rm NS}/N_{\rm tot})^{0.8}$ of the neutron-star accretion efficiency, a comparable number of each may be detectable. We make predictions for the number of isolated accreting black holes in our Galaxy that can be detected with X-ray surveys as a function of efficiency, concluding that all-sky surveys at a depth of $F = F_{-15} 10^{-15}\,{\rm erg\,cm^{-2}\,s^{-1}\,dex^{-1}}$ can find $N(>F) \sim 10^4 N_9 (F_{-15}/\epsilon_{-5})^{-1.2}$ isolated accreting black holes for a velocity dispersion of $40\,{\rm km\,s^{-1}}$ and an X-ray accretion efficiency of $\epsilon = \epsilon_{-5} 10^{-5}$. Deeper surveys of the Galactic plane with *Chandra* or *XMM-Newton* may find tens of these objects per year, depending on the efficiency. We argue that a mass estimate can be derived for microlensing black hole candidates with an X-ray detection.

Key words: accretion, accretion discs – black hole physics – Galaxy: stellar content – X-rays: ISM – X-rays: stars.

1 INTRODUCTION

A black hole may be detected only via its interactions with surrounding matter or light. Black holes in binary-star systems are strong and transient X-ray sources fed by accretion from a stellar companion. However, isolated black holes – that is, black holes without companions or black holes in wide binaries – can easily escape detection. These may constitute the majority of the population of black holes, since the fraction in close binaries with $a < 100\,{\rm au}$ is ~ 0.01 based on stellar evolution calculations for massive star binaries (Chris Fryer, private communication). Young isolated neutron stars are much easier to detect as pulsars, but once the magnetic field, spin, and thermal energy decay away, an old neutron star becomes as invisible as a black hole. Several authors (Ostriker, Rees & Silk 1970; Treves & Colpi 1991; Blaes & Madau 1993) have proposed searching for isolated old neutron stars lit up by accreting matter from the interstellar medium (ISM). A tenth of the rest-mass energy of the accreting gas can be directly converted to luminosity, assuming that all the accreted material is thermalized as it hits the neutron-star surface. These predictions motivated searches that turned up several isolated neutron-star candidates (Stocke et al. 1995; Walter, Wolk & Neuhauser 1996; Wang 1997; Schwope et al. 1999); however, it is possible that these are young cooling neutron stars powered by processes other than accretion (Treves et al. 2000).

The known Galactic black hole X-ray-binary population has a velocity dispersion smaller by a factor of ~ 5 than neutron stars (van Paradijs & White 1995; White & van Paradijs 1996, hereafter WvP; Hansen & Phinney 1997) and an average mass larger by a factor of ~ 6 (see below, and also Bailyn et al. 1998 and Thorsett & Chakrabarty 1999). The accretion rate for an object of mass M accreting from the ISM is determined by the Bondi–Hoyle formula (Bondi & Hoyle 1944),

$$\dot{M} = \frac{\lambda 4\pi G^2 M^2 n \mu}{(v^2 + c_{\rm s}^2)^{3/2}}, \qquad (1)$$

where v is the velocity of the black hole with respect to the local ISM, n is the number density of hydrogen in the ISM, $\mu = \rho/n$ where ρ is the particle mass density, $c_{\rm s}$ is the sound speed of the ISM, and λ is a parameter of order unity (we set $\lambda = 1$ hereafter).

★E-mail: agol@tapir.caltech.edu
†Chandra Fellow.

Assuming that isolated black holes have the same mass range and velocity dispersion as black holes in X-ray binaries, one would expect the typical accretion rate on to isolated black holes from the ISM to be larger by a factor of $\sim 4 \times 10^3$ compared to neutron stars. The expected detection rate of isolated black holes accreting from the ISM may be reduced, as the number of black holes in our Galaxy may be smaller by a factor of ~ 10 than the number of neutron stars, and the lack of a hard surface may result in lower luminosities for black holes accreting at small accretion rates. Garcia et al. (2001) argue that black holes have quiescent X-ray efficiencies $\sim 10^{-2}$ of neutron stars; however, Bildsten & Rutledge (2000) argue that the detected X-rays may have nothing to do with accretion, and that V404 Cyg is an exception to this rule, indicating that there may be a wide range of accretion efficiencies. If black holes do have a reduced efficiency compared to neutron stars, this reduction can be compensated by the larger accretion rates and the smaller scaleheight of black holes which increases their number density in the mid-plane where most of the interstellar gas mass is located. The accretion rate of neutron stars can be suppressed by interactions with the magnetic field if the magnetic field decays on a 10^{8-9} yr time-scale (Colpi et al. 1998; Livio, Xu & Frank 1998), while black holes do not have an intrinsic magnetic field, so accretion can proceed uninhibited by magnetic pressure or torque. Thus we are motivated to compute the expected numbers and accretion rates of isolated black holes in our Galaxy.

The problem of black holes accreting from the ISM has been considered by several authors. We approach the problem in a different way from previous authors (listed below) by using the properties of black hole X-ray binaries to constrain the phase-space distribution of black holes within the entire Galactic disc, while considering the properties of all phases of the ISM, deriving the distribution of accretion rates including radiative pre-heating, and finally deriving the distribution of X-ray fluxes. Grindlay (1978) considered spherical-accretion models for X-ray sources now known to be accreting from companions. Carr (1979) estimated the luminosity of black holes in the Galactic disc, but did not predict their detection probability. McDowell (1985) computed the visual and infrared fluxes of black holes accreting spherically from molecular clouds, but only out to 150 pc. Campana & Pardi (1993) computed the fluxes of black holes within the disc of the Galaxy accreting spherically from molecular clouds, without computing the probability distribution of accretion rates. Heckler & Kolb (1996) computed the fluxes of a putative halo population of black holes accreting spherically while passing within 10 pc of the Sun. The large velocities, low densities, and large scaleheights of a halo population greatly reduce the number of black holes at a given accretion rate. Popov & Prokhorov (1998) took into account the spatial distribution of the warm ISM, assuming that the black holes receive a kick velocity at birth of $\sim 200\,\mathrm{km\,s^{-1}}$, which greatly reduces the accretion rates. Fujita et al. (1998) computed the fluxes of black holes in the disc accreting via an advection-dominated accretion flow at a distance of 400 pc (the Orion cloud) for a few velocities, without computing the full probability distribution. Grindlay et al. (2001) estimate that of order 10^3 black holes in molecular clouds might be detectable by the proposed *Energetic X-ray Imaging Survey Telescope* (*EXIST*) experiment based on an accretion efficiency of 10^{-2}.

The spectrum of an accreting black hole has been computed in the spherical-accretion limit (Ipser & Price 1977, 1982, 1983); however, as we show below, the accreted material will possess non-zero angular momentum, possibly forming an accretion disc which may increase the efficiency of accretion. Thus we parametrize our results in terms of the unknown accretion efficiency.

In Section 2 we summarize the known properties of binary black holes and their distribution in phase-space. In Section 3 we estimate the accreted angular momentum, and discuss the range of accretion efficiencies and the effects of radiative feedback. In Section 4 we discuss the properties of the ISM necessary for computing the accretion rates of black holes. In Section 5 we compute the distribution of accretion rates and luminosities for black holes within the disc of the Galaxy. In Section 6 we estimate the detection rates of black holes under the persistent and transient assumptions, and then predict the fluxes as a function of distance for the three candidate black-hole microlenses. Finally, in Section 7 we summarize our conclusions.

2 BLACK HOLES IN OUR GALAXY

Here we summarize the properties of black holes in X-ray binaries, which we will use to describe the isolated black hole distribution as well.

2.1 Number of black holes

Estimating the number of stellar remnant black holes in the Milky Way requires knowing the star formation history, the initial mass function, and the fraction of stars which evolve into black holes as a function of metallicity. Simple estimates based on the expected number of black-hole to neutron-star remnants indicate about 10^8 black holes (Shapiro & Teukolsky 1983; van den Heuvel 1992). Chemical enrichment by supernovae within the Milky Way indicates about $\sim 2 \times 10^8$ black holes should have formed (Samland 1998). The MACHO and OGLE groups claim to have three detected isolated black holes via gravitational microlensing (Bennett et al. 2001; Mao et al. 2002). The mass of these lenses is inferred only statistically, so these events may be due to more distant, low-mass stars; nevertheless, these three events indicate that at most $\sim 10^9$ black holes reside in the Milky Way disc (Agol et al. 2002).

2.2 Phase-space distribution of black holes

WvP have estimated that the rms distance from the Galactic plane for black hole X-ray binaries, $z_{\rm rms}$, is about 450 pc, which corresponds to a scaleheight of $H \sim 320$ pc and a velocity dispersion of $\sigma_v \sim 40\,\mathrm{km\,s^{-1}}$. This is consistent with the radial velocity measurements of low-mass black hole X-ray binaries when corrected for Galactic rotation (Brandt, Podsiadlowski & Sigurdsson 1995; Nelemans, Tauris & van den Heuvel 1999), with the exceptions of GRS 1655−40, which has $v_r = -114\,\mathrm{km\,s^{-1}}$, and J1118+480, which has $v \sim 145\,\mathrm{km\,s^{-1}}$ with respect to the local standard of rest (Mirabel et al. 2001). Thus there appear to be two black hole populations with low and high velocity dispersions as there are of neutron stars (Cordes & Chernoff 1998). Only the low-velocity objects will be detectable by accretion, so we simply consider this population. We have estimated the scaleheight of black hole X-ray binaries using a maximum-likelihood estimator $\mathrm{d}p/\mathrm{d}H = \Pi_i \exp(-|z_i|/H)/(2H)$, where H is the disc scaleheight and z_i is the height above the disc, given the distances listed in Table 1. The resulting probability distribution is shown in Fig. 1. We measure a scaleheight of $H = 370^{+130}_{-60}$ pc (1σ) and, at 90 per cent confidence, $270 < H < 590$ pc. This scaleheight is consistent with a population with a velocity dispersion in the z-direction of

Table 1. Height distribution of black hole X-ray binaries.

Name	l°	b°	D(kpc)	z(pc)	Ref.
0422+32	165.9	−11.9	2.2	−453	CSL
0620−00	210.0	−6.5	0.8	−91	CSL
1009−45	275.9	9.3	3.0	485	CSL
1118+48	157.7	62.3	1.9	1682	Mirabel et al. (2001)
1124−68	295.3	−7.1	5.5	−680	CSL
1524−62	320.3	−4.4	4.4	−338	CSL
1543−47	330.9	5.4	9.1	856	Orosz et al. (1998)
1550−564	325.9	−1.8	2.5	79	Wilson & Done (2001)
1655−40	345.0	2.5	3.2	140	CSL
1658−48	338.9	−4.3	3.0	−225	Fender (2001)
1705−25	358.6	9.1	4.3	680	CSL
1719−24	0.1	7.0	2.4	292	CSL
1740.7−2942	359.1	−0.1	8.5	−15	WvP
1758−258	4.5	−1.4	8.5	207	Fender (2001)
1846−031	30.0	−0.9	7.0	−110	WvP
1915+105	45.3	−0.9	12.5	−196	CSL
1958+35	1.3	3.1	2.	108	Fender (2001)
2000+25	63.4	−3.0	2.5	−131	WvP
2023+33	73.2	−2.1	3.5	−214	WvP

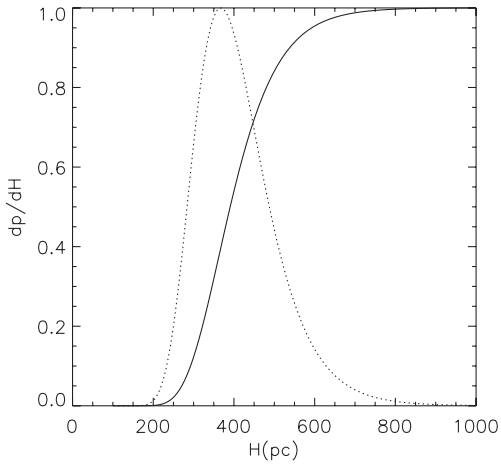

Figure 1. The probability distribution of scaleheights for black hole X-ray binaries, given the observed heights of the 19 black hole X-ray binaries listed in Table 1.

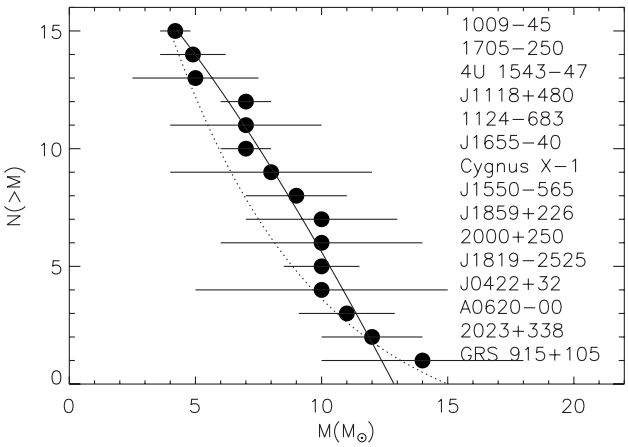

Figure 2. The number of black holes with masses above M, $N(>M)$ versus mass. The solid curve is the best-fitting distribution function, while the dotted curve is the theoretical distribution from Fryer & Kalogera (2001).

$\sim 15-20\,\mathrm{km\,s^{-1}}$. Since black holes in X-ray binaries are the only sure detections of stellar-mass black holes, we will assume that this scaleheight and velocity dispersion apply to isolated black holes as well.

2.3 Mass distribution of black holes

The measured masses for black hole X-ray binaries (see, e.g., Narayan, Garcia & McClintock 2002 for a recent compilation) are plotted as $N(>M)$ in Fig. 2. We have then fitted a power-law mass distribution,

$$\mathrm{d}N/\mathrm{d}M = n_M M^{-\gamma}, \tag{2}$$

with a lower mass cut-off at M_1 and an upper mass cut-off at M_2. We obtain a best fit for $\gamma = -0.35$, $M_1 = 4\,\mathrm{M}_\odot$, and $M_2 = 13\,\mathrm{M}_\odot$. The average mass of the distribution is $\sim 9\,\mathrm{M}_\odot$, close to the mean of the data $\langle M\rangle = 9.6\,\mathrm{M}_\odot$. We have normalized this to unity, $n_M = (\gamma-1)/(M_1^{1-\gamma} - M_2^{1-\gamma})$, and we assume that it applies throughout the Galaxy.

3 EFFICIENCY OF ACCRETION

The Bondi–Hoyle formula may be appropriate for computing the accretion rate, but we must then convert that accretion rate into an observable luminosity in some band with some efficiency, ϵ. To do so requires a detailed model for the accretion flow; we side-step this problem by parametrizing our results with ϵ. However, we first need to consider what values ϵ might take.

3.1 Angular momentum of accreted material

If the accreting gas were perfectly uniform, then the accreted angular momentum is quite small, and the accretion flow follows a one-dimensional supersonic solution, for which the luminosity can be predicted (Ipser & Price 1977; Shapiro & Teukolsky 1983). However, small perturbations in the density or velocity of the accreting gas will lead to an angular momentum large enough to circularize gas before it accretes (Shapiro & Lightman 1976). If there is a gradient in the density field that is perpendicular to the direction of motion of the black hole, then the accreted angular

momentum scales as

$$l = \frac{1}{4}\frac{\Delta\rho}{\rho} v r_{\rm A}, \tag{3}$$

where $\Delta\rho$ is the difference in density between the top and bottom of the accretion cylinder, and $r_{\rm A} = GM/(v^2 + c_s^2)$ is the accretion radius. Numerical simulations confirm that this formula is correct to order of magnitude (Ruffert 1999). The observed density fluctuations in our Galaxy scale as $\delta\rho/\rho \sim (L/10^{18}\,{\rm cm})^{1/3}$ (Armstrong, Rickett & Spangler 1995), extending down to a scale of $\sim 10^8$ cm. The exponent of this scaling is nearly consistent with a Kolmogorov spectrum of density (Dubinski, Narayan & Phillips 1995). Evaluating this at $L = 2r_{\rm A}$, we can then find the radius of the resulting accretion disc, $r_{\rm disc}$, by equating the angular momentum of the gas with the Keplerian angular momentum due to the black hole, $l_{\rm Kep} = \sqrt{GMr_{\rm disc}}$. This gives

$$\frac{r_{\rm disc}}{r_{\rm g}} = 10^4 \left(\frac{M}{9\,{\rm M}_\odot}\right)^{2/3} \left(\frac{\sqrt{v^2 + c_s^2}}{40\,{\rm km\,s^{-1}}}\right)^{-10/3}. \tag{4}$$

So we see that a disc will almost always form in interstellar accretion (though not necessarily a radiative-efficient thin disc). A similar argument is given in Fujita et al. (1998) for the case of molecular clouds, for which the slope of velocity fluctuations is similar to that expected by a Kolmogorov spectrum (Larson 1981). The neutral ISM seems to follow a power law with a similar slope and normalization (Lazarian & Pogosyan 2000), which will also lead to non-zero accreted angular momentum; however, the length-scales probed in molecular and atomic gas are much larger than the scale of the accretion radius.

The accretion time-scale for the disc scales as $t_{\rm d} = \alpha_{\rm SS}^{-1}(GM/r_{\rm disc}^3)^{-1/2}(r_{\rm disc}/h)^2$, where h is the height of the disc, and $\alpha_{\rm SS}$ is the ratio of the viscous stress to the pressure in the disc. If the velocity and density fields of the ISM are incoherent on the scale of these fluctuations, then the angular momentum can change on a time-scale of $t_{\rm a} = r_{\rm A}/v$, as gas will be accreted with the angular momentum vector pointing in a different direction after this time-scale. Thus the angular momentum of the disc can be reduced due to a random walk of the accreted angular momentum vector if $t_{\rm A} \ll t_{\rm d}$. We estimate

$$\frac{t_{\rm d}}{t_{\rm a}} \sim 2\frac{r_{\rm A}}{2\times 10^{13}\,{\rm cm}} \left(\frac{0.1r}{h}\right)^2 \left(\frac{\alpha_{\rm SS}}{0.1}\right)^{-1}, \tag{5}$$

which indicates that there may be only a slight reduction in the angular momentum since these time-scales are comparable. The residual angular momentum means that we *cannot* use spherical-accretion formulae for the luminosity, but we must estimate the efficiency of the accretion disc that forms.

3.2 Range of efficiencies

We assume that the black holes radiate a spectrum with spectral index $\alpha = 1$, where $F_\nu \propto \nu^{-\alpha}$, consistent with the typical spectrum of black hole X-ray binaries in quiescence (Kong et al. 2002), so that equal energy is emitted per unit decade of energy. We define $L_{\rm ion}$ as the luminosity from 1 to 1000 Ryd (13.6 eV), so the efficiency is $\epsilon_{\rm ion} = L_{\rm ion}/(\dot{M}c^2)$. Estimates of the accretion rate in Cygnus X-1 indicate that it is accreting with an X-ray efficiency of $\epsilon_{\rm ion} \sim 10^{-1}$ (Shapiro & Teukolsky 1983). However, at low accretion rates the density of the gas decreases, reducing the cooling rate so that it may not be able to cool, resulting in a radiative efficiency much lower than the ~ 10 per cent available due to gravitational potential energy (Narayan & Yi 1994). We again appeal to black hole X-ray binaries. By estimating the mass accretion rates in black hole X-ray binaries and X-ray luminosities in the quiescent state, Lasota (2000) concludes that the 2–10 keV efficiency is about 2×10^{-6}, assuming that this luminosity is solely due to accretion, implying $\epsilon_{\rm ion} \sim 10^{-5}$. Low upper limits on the X-ray Bondi-accretion efficiencies are inferred for some supermassive black holes in elliptical galaxies (Loewenstein et al. 2001). The Galactic Centre black hole has an X-ray efficiency of $\sim 4\times 10^{-8}$–2×10^{-6} in the 2–10 keV band for a Bondi–Hoyle accretion rate of $10^{-6}\,{\rm M}_\odot\,{\rm yr}^{-1}$ (Baganoff et al. 2001), but it may have been much brighter within the last ~ 100 years (Koyama et al. 1996). Thus we parametrize our results in terms of an unknown X-ray efficiency, using 10^{-5} as the fiducial efficiency.

For certain ranges of parameters, the disc may be unstable to the hydrogen-ionization disc instability (Lasota 2001), creating intermittent outbursts of higher luminosity between long periods of quiescence, with changes in luminosity of 10^5. We will discuss the possible effect this may have on the number of detectable sources in Section 6.2.

3.3 Radiative feedback

The gas in the vicinity of the black hole will be heated by the ionizing radiation field produced by accretion. If the temperature rises enough, then the accretion radius, and thus the accretion rate, will decrease (Shvartsman 1971; Ostriker et al. 1976). For an $\alpha = 1$ spectrum, the mean opacity from 1–1000 Ryd of neutral gas with cosmic abundance is $\sigma_{\rm cold} = 3.87\times 10^{-18}\,{\rm cm}^2$ per hydrogen atom. The heating rate is then given by $H = L_{\rm x} n_{\rm H}\sigma_{\rm cold}/(4\pi R^2)$, where R is the distance from the black hole. For temperatures lower than $\sim 10^4$ K and for a small ratio of radiation energy density to gas energy density, the heating rate greatly exceeds the cooling rate. Consider a fluid element directly in front of the path of a moving black hole. As the black hole approaches with velocity v, the ratio of the total heating rate to the initial energy density, e_0, of the gas is

$$\frac{e_{\rm tot}}{e_0} = \frac{1}{e_0}\int_R^\infty {\rm d}RH/v = 2\times 10^5 \epsilon_{\rm ion} v_{40}^{-2}(r/r_{\rm A})T_4^{-1}, \tag{6}$$

where $e_{\rm tot}$ is the total energy density absorbed by a fluid element (neglecting cooling), $v = v_{40}40\,{\rm km\,s^{-1}}$ and $T = T_4 10^4$ K. Thus, even for small efficiencies the gas is strongly heated outside the accretion radius. Once H and He are ionized, the mean opacity drops by three orders of magnitude, and the gas remains at around 2×10^4 K. This has been confirmed by detailed numerical simulations by Blaes, Warren & Madau (1995). Above this temperature, the cooling and heating times become much longer than the accretion time, so the gas falls in adiabatically. Thus we take the temperature of the accreted gas to be $T_0 = 2\times 10^4$ K for all phases of the ISM except the hot H II.

4 GAS IN OUR GALAXY

4.1 Phases of the ISM

The interstellar medium in our Galaxy consists of at least five identifiable phases (Bland-Hawthorn & Reynolds 2000) in approximate pressure equilibrium, $P \sim 2\times 10^3 k_{\rm B}$, where $k_{\rm B}$ is the Boltzmann constant. The highest accretion rates will occur in the regions of the highest density. This means that the observable sources will be dominated by the giant molecular clouds (GMCs)

consisting mostly of H_2 ($T \sim 10\,K$) and the cold neutral medium (CNM) consisting of H I clouds ($T \sim 10^2\,K$). These phases comprise approximately 40 and 50 per cent of the total mass of gas in our Galaxy.

The warm neutral and ionized components ($T \sim 8000\,K$) of the ISM have densities that are $\sim 10^{-2}$ of the CNM, so the maximum accretion rates are $\sim 10^{-2}$ times smaller than the maximum for the CNM, while the hot component of the ISM ($T \sim 10^6\,K$) has a density $\sim 10^{-2}$ of the warm components, reducing the maximum accretion rate by another factor of 10^{-2}. However, these phases fill a much larger volume in the ISM, and thus should be considered.

We next refine the above estimates by considering the distribution of each phase as a function of number density.

4.2 Filling fraction of the ISM

To estimate the distribution of accretion rates for black holes in our Galaxy, we need to know the volume of the Galaxy filled by gas of a given number density. We define this as

$$\frac{df}{dn} = f_0 n^{-\beta}, \tag{7}$$

where df/dn is the fraction of volume filled by gas with number density between n and $n + dn$, and f_0 is a normalization constant. Berkhuijsen (1999) has shown that $\beta_{GMC} \sim 2.8$, while $\beta_{CNM} \sim 3.8$. This can be seen for the molecular clouds by noting that the mass function of molecular clouds in our Galaxy scales as $dN/dM \propto M^{-1.6}$ (Dickey & Garwood 1989), while the number density of clouds scales with size, D, as $n \propto D^{-1}$ (Larson 1981; Scoville & Sanders 1987). Assuming that clouds have a spherical volume, one finds $df/dn \propto V(dM/dn)(dN/dM) \propto n^{-2.8}$. Since the number density–size relation is derived for the average density of clouds, β may be slightly smaller because each cloud may contain regions where the gas density is higher than average.

We assume that the GMCs span number densities from $n_1 = 10^2\,cm^{-3}$ to $n_2 = 10^5\,cm^{-3}$, while the CNM spans number densities from $n_1 = 10\,cm^{-3}$ to $n_2 = 10^2\,cm^{-3}$. Finally, we assume that the scaleheight of the molecular clouds is 75 pc, while the scaleheight of the CNM is 150 pc; we also assume that all phases are axisymmetric.

The surface mass density of molecular gas as a function of radius is taken from Scoville & Sanders (1987) and Clemens, Sanders & Scoville (1988), while we assume the distribution of the CNM to be constant with $\Sigma = 4.5\,M_\odot\,pc^{-2}$ for $R > 4$ kpc, and zero inside 4 kpc (Scoville & Sanders 1987). The molecular-gas surface density has a strong peak at the Galactic Centre, and another peak around 5 kpc from the Galactic Centre; then it decreases outwards (Scoville & Sanders 1987). We ignore variations of the surface density in azimuth, and we approximate the distribution in z as an exponential, $f_0(z) = f_0(0)\exp(-|z|/H)$. From these surface densities, we compute the filling fraction in the mid-plane as

$$f_0(0) = \frac{\Sigma(\beta-2)(n_1^{1-\beta} - n_2^{1-\beta})}{2H\mu(\beta-1)(n_1^{2-\beta} - n_2^{2-\beta})}, \tag{8}$$

where $\mu = 2.72 m_p$ for the GMC, and $\mu = 1.36 m_p$ for the CNM. At the solar circle, this gives $f_0(\mathrm{GMC}) = 10^{-3}$, while $f_0(\mathrm{CNM}) = 0.04$.

The warm H I, warm H II, and hot H II we take as constant densities of 0.3, 0.15 and $0.002\,cm^{-3}$ respectively, mid-plane filling factors of 35, 20 and 40 per cent, as well as scaleheights of 0.5, 1 and 3 kpc (Bland-Hawthorn & Reynolds 2000). We assume that the hot H II has a temperature of $10^6\,K$, and thus $c_s = 150\,km\,s^{-1}$. The corresponding surface mass densities are 4, 2 and $0.2\,M_\odot\,pc^{-2}$ respectively, which we assume to be constant as a function of Galactic radius.

5 ACCRETION RATE AND LUMINOSITY DISTRIBUTION FUNCTIONS

The distribution function of mass-accretion rate for black holes located at a given region in the Galaxy is given by

$$\frac{d^2N}{d\dot{M}\,dV} = \int_{M_1}^{M_2} dM \int_{n_1}^{n_2} dn \int_0^\infty dv \frac{df}{dn}\frac{d^2n_{BH}}{dM\,dv}\,\delta[\dot{M}(n,M,v) - \dot{M}], \tag{9}$$

where dV is the volume element and

$$\frac{d^2n_{BH}}{dM\,dv} = N_{BH}(R,z)\sqrt{\frac{2}{\pi}}\frac{v^2}{\sigma_v^3}\exp\left(-\frac{v^2}{2\sigma_v^2}\right) n_M M^{-\gamma}. \tag{10}$$

We define $\dot{M}_0 = \pi G^2 M_\odot^2 m_p (1\,km\,s^{-1})^{-3} = 3.8 \times 10^{14}$, so that $\dot{M}(n,M,v) = \dot{M}_0 n M^2 (v^2 + c_s^2)^{-3/2}$. For a given mass and sound speed, we can define the minimum number density required for accretion at a rate greater than $\dot{M}$: $n > n_0 = \dot{M}c_s^3/(\dot{M}_0 M^2)$. Using equations (1) and (2), we can first carry out the v integration analytically,

$$\begin{aligned}\frac{d^2N}{d\dot{M}\,dV} = N_{BH}\int_{M_1}^{M_2} dM n_M M^{-\gamma} \int_{\max\{n_1,n_0\}}^{\max\{n_2,n_0\}} dn f_0 n^{-\beta} \\ \times \sqrt{\frac{2}{\pi}}\frac{v_0}{\sigma_v^3}\frac{(\dot{M}_0 n M^2)^{2/3}}{\dot{M}^{5/3}}\exp\left(-\frac{v_0^2}{2\sigma_v^2}\right),\end{aligned} \tag{11}$$

where $v_0^2 = (\dot{M}_0 n M^2/\dot{M})^{2/3} - c_s^2$. The remaining two integrals are computed numerically.

In Fig. 3 we plot the function $dN/d\dot{M}$ for the various phases of the ISM at the solar circle. The densest gas (GMCs) dominates the highest accretion rates, while the hottest gas dominates the lowest accretion rates. For the hot H II, accretion is subsonic and n is assumed to be constant, so $\dot{M} \propto M^2$. Thus, $dN/d\dot{M} \propto \dot{M}^{-(1+\gamma)/2}$,

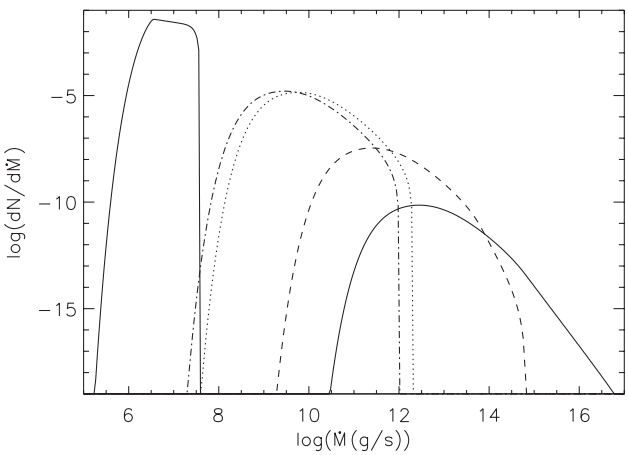

Figure 3. The number density ($kpc^{-3}\,g^{-1}\,s$) of black holes accreting with accretion rates between $\dot{M}$ and $\dot{M} + d\dot{M}$ as a function of $\dot{M}$ at the solar radius for $\sigma_v = 40\,km\,s^{-1}$. The solid curve refers to black holes accreting within molecular clouds, while the short-dashed curve refers to black holes within the cold neutral medium. The dotted curve is for black holes within the warm H I, the dot-dashed curve for the warm H II, and the dash-triple-dot curve for the hot H II.

spanning a range in $\dot{M}$ of $(M_2/M_1)^2$. The other phases have more complicated accretion-rate distributions, since $\sigma_v > c_s$.

To compute the expected total number of black holes in the Galaxy accreting at a rate $\dot{M}$, we integrate the luminosity functions (assumed to be constant) over the gas filling fraction times the number density of black holes as a function of position over the entire Galaxy,

$$\frac{dN}{d\dot{M}} = \left.\frac{d^2N}{d\dot{M}\,dV}\right|_{(R_\odot,z=0)} \int_0^\infty dR 2\pi R \exp\left(-\frac{R-R_\odot}{R_{\rm disc}}\right) 2\frac{\Sigma(R)}{\Sigma(R_\odot)} \times \int_0^\infty dz \exp\left(-\frac{z}{H_{\rm BH}} - \frac{z}{H_{\rm gas}}\right). \quad (12)$$

Fig. 4(a) shows $N(>\dot{M}) = \int_{\dot{M}}^\infty d\dot{M}'(dN/d\dot{M}')$ for both black holes and neutron stars. For neutron stars, we choose $M = 1.4\,M_\odot$, 86 per cent with $\sigma_v = 175\,{\rm km\,s^{-1}}$ and 14 per cent with $\sigma_v = 700\,{\rm km\,s^{-1}}$ (Cordes & Chernoff 1998), $N_\odot = 5.2\times10^5\,{\rm kpc^{-3}}$, and $H = 1\,{\rm kpc}$, yielding a total of 10^9 neutron stars within our Galaxy. We have ignored suppression of accretion by magnetic effects, noting that this may reduce the number of observable neutrons stars by a factor of ~ 5 below what we have computed (Colpi et al. 1998; Livio et al. 1998). The total number of accreting black holes is smaller than the total number in the disc, since we have assumed that the gas filling factor decreases with scaleheight. This reduction may be artificial, since gas at some density presumably fills the entire Galaxy, but this affects only small accretion rates.

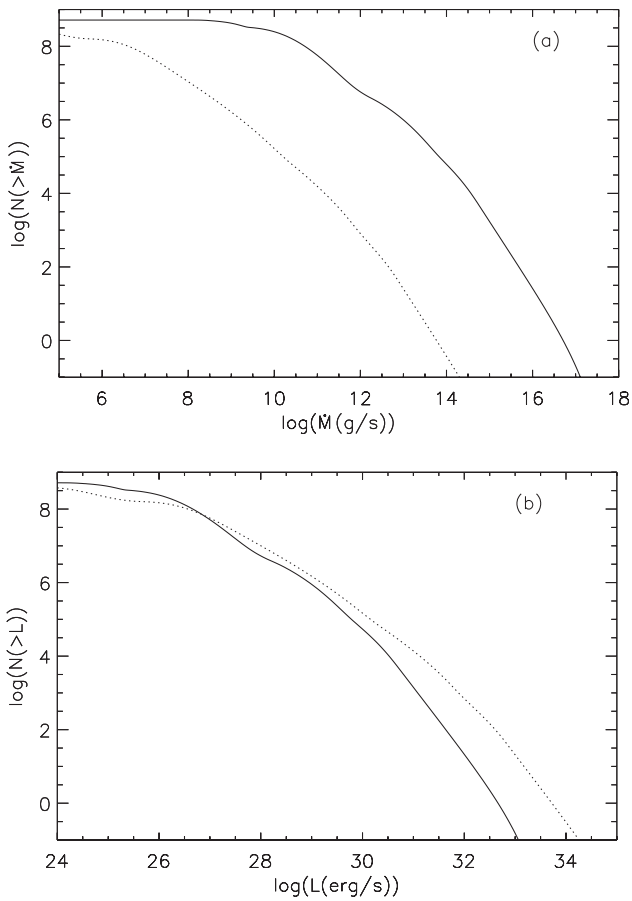

Figure 4. (a) The number of black holes in the Milky Way with accretion rates greater than $\dot{M}$ for $\sigma_v = 40\,{\rm km\,s^{-1}}$ (solid line). For comparison, the dotted line shows the same computation for neutron stars. (b) The number of black holes in the Milky Way with luminosities greater than $L_{\rm ion}$ with $\epsilon_{\rm ion} = 10^{-5}$ (solid line) and the number of neutron stars for $\epsilon_{\rm ion} = 10^{-1}$ (dotted line).

We expect $\sim 10^3 N_9$ isolated black holes to be accreting at rates comparable to the estimated rates in black hole X-ray binaries, $\dot{M} > 10^{15}\,{\rm g\,s^{-1}}$ (van Paradijs 1996). This is comparable to the parent population of black hole X-ray binaries, which may be 10^{2-3} (Iben, Tutukov & Yungelson 1995). Black holes outnumber neutron stars due to their larger mass and smaller space velocity, as shown in Fig. 4(a).

To compute the number of detectable isolated black holes requires converting the accretion-rate distribution into a luminosity function. Given the uncertainties in accretion physics, we will make two assumptions based on what is known about black hole X-ray binaries: persistent and transient sources. The first assumption, shown in Fig. 4(b), is that the sources are time-steady, similar to high-mass X-ray binaries such as Cygnus X-1. Under this assumption, we simply convert the accretion rate into an X-ray luminosity in a given X-ray band. Shown is the ionizing radiation band from 1 to 1000 Ryd for $\epsilon_{\rm ion} = 10^{-5}$; the horizontal axis simply scales with efficiency. The black hole and neutron-star functions overlap for $\epsilon_{\rm ion} \sim 10^{-5}$, despite the lower black hole efficiency due to the larger black hole mass, smaller velocity dispersion, and smaller scaleheight. The total ionizing luminosity of isolated accreting black holes within the Milky Way is $\sim 10^{36} N_9 \epsilon_{-5}\,{\rm erg\,s^{-1}}$.

The second assumption that the black holes are transient will be discussed in Section 6.2.

6 DETECTION PROBABILITY

To compute the detection probability, we need to integrate the number of sources above a given observed flux as a function of position within the Galaxy. We will consider two energy emission bands, 'soft' X-ray from 1 to 10 keV, and 'hard' X-ray from 10 to 100 keV, which have efficiencies of $\epsilon_{\rm soft}$ and $\epsilon_{\rm hard}$. Since the model spectrum we have used is flat, $\nu f_\nu \propto \nu^0$, the luminosity per unit decade of photon energy is constant. Thus the flux in each of these bands is 1/3 of the flux of ionizing photons which covers three decades, or $\epsilon_{\rm soft} = \epsilon_{\rm hard} = \epsilon_{\rm ion}/3$. A more complex X-ray spectrum will change our results by factors of order unity, which we defer to future work, given the poor theoretical understanding of the spectra of accreting black holes.

For neutron stars, we assume a spectrum composed of a blackbody with $T = 0.15\,{\rm keV}$ plus a power law with $\alpha = 1$ (i.e., flat in νF_ν) and the flux from 1 to 10 keV equal to 1 per cent of the total flux of the blackbody component. This was chosen to be similar to the spectra of neutron-star binaries Cen X-4 and Aquila X-1 in quiescence (Rutledge et al. 2001a,b). This spectrum yields $\epsilon_{\rm soft} = 0.13\epsilon_{\rm ion}$ and $\epsilon_{\rm hard} = 0.03\epsilon_{\rm ion}$, because most of the flux is in the extreme ultraviolet. We neglect photoelectric absorption, since the half-column density of molecular clouds is approximately $N_{\rm H} \sim 1\times10^{22}\,{\rm cm^{-2}}$, which leads to absorption of only 36 per cent of the flux in the soft X-ray band (using the opacities of Morrison & McCammon 1987). Toward the Galactic Centre, the hydrogen column density is about $N_{\rm H} \sim 6\times10^{22}\,{\rm cm^{-2}}$ due to the ring of gas near the centre, leading to absorption of about 86 per cent of the soft flux. In the hard X-ray band, the absorption is negligible.

6.1 Persistent sources

For the persistent-source assumption, we assume that the accretion flow emits isotropically, so we simply need to integrate the

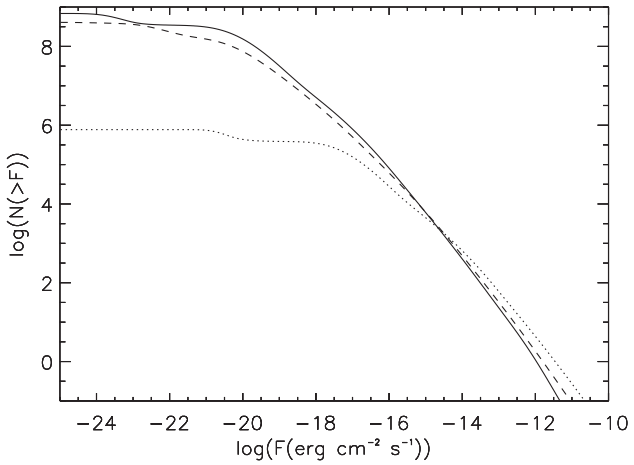

Figure 5. The number of black holes visible to an observer located within the Solar system as a function of X-ray flux in the soft or hard band for a persistent accretion efficiency of $\epsilon_{\rm ion} = 10^{-5}$ with $\epsilon_{\rm soft,hard} = \epsilon_{\rm ion}/3$ (solid line).For comparison, the number of neutron stars above a given soft X-ray flux is also shown in the soft X-ray band with $\epsilon_{\rm soft} = 0.13\epsilon_{\rm ion} = 0.013$ (dotted line). In addition, we show predictions for a population of 10^6 black holes with mass $250\,{\rm M}_\odot$ for efficiencies of 10^{-5} (dot-dashed line). Note that the horizontal axis scales with efficiency for each object.

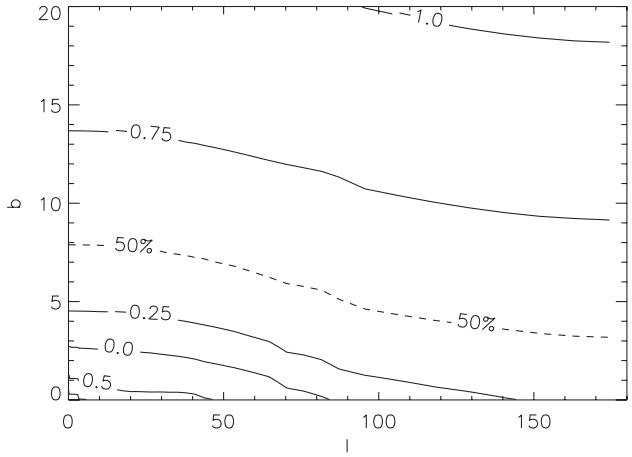

Figure 6. The logarithm of the number density of black holes per degree square with fluxes above $F_{\rm X} = 10^{-15}\epsilon_{-5}\,{\rm erg\,cm^{-2}\,s^{-1}}$ in the soft or hard band as a function of Galactic longitude, $l(^\circ)$, and latitude, $b(^\circ)$. The labels indicate the logarithm of the number density. The dashed line indicates the contour within which 50 per cent of the black holes are contained. The total number of black holes above this flux level is $\sim$3000, while the maximum number density is 18 per square degree at the Galactic Centre.

luminosity function over the entire Galaxy with the transformation

$$\frac{{\rm d}N}{{\rm d}F\,{\rm d}V} = \frac{{\rm d}N}{{\rm d}\dot{M}\,{\rm d}V}\frac{4\pi D^2}{\epsilon_{\rm soft,hard}c^2}, \qquad (13)$$

where D is the distance to a given point in the Galaxy. Fig. 5 shows the predicted number of sources as a function of flux integrated over the entire Galaxy for the persistent-source assumption. Despite the much lower assumed efficiency, the number of detectable black holes becomes comparable to the number of detectable neutron stars for $\epsilon_{\rm BH} \sim 10^{-4}\epsilon_{\rm NS}(N_{\rm BH}/N_{\rm NS})^{0.8}$. The number of black holes above a certain flux at high flux scales approximately as $N(>F) = 6\times10^3F^{-1.2}$ near $F = 10^{-15}\epsilon_{-5}\,{\rm erg\,cm^{-2}\,s^{-1}}$. Given the flatness of this dependence, the best detection strategy is to cover as much area of the sky as possible, assuming the constraint of a fixed amount of observing time with an X-ray telescope with a sensitivity that scales as $t^{-1/2}$.

We have also computed the number density of black holes with fluxes greater than $10^{-15}\epsilon_{-5}\,{\rm erg\,cm^{-2}\,s^{-1}}$ as a function of Galactic latitude and longitude for one quadrant of the Galaxy (Fig. 6). The black holes are strongly concentrated toward the Galactic plane and toward the Galactic Centre. Half of the black holes lie within the dashed contour, which covers an area of $1000\,{\rm deg}^2$ in Fig. 6 (one quadrant of the Galaxy), giving an average of $0.7N_9$ per square degree within this region near the Galactic plane. We have not attempted to include the inhomogeneity of the ISM, which might be important for nearby black holes in the local bubble or for black holes in interstellar clouds.

Finally, we have computed the distribution of sources with distance from the Sun. Fig. 7 shows the number of black hole sources with fluxes greater than $F = 10^{-15}\epsilon_{-5}\,{\rm erg\,cm^{-2}\,s^{-1}}$ less than a given distance for each of the phases of the ISM. The total number of sources above this flux level is $1900N_9$ in the GMCs, $3800N_9$ in the CNM, $300N_9$ in the warm H I, $70N_9$ in the warm H II, and 0 in the hot H II. The average distance for the detectable black holes is 2.7 kpc in the GMCs, 0.4 kpc in the CNM, 70 pc in the warm H I, and 50 pc in the warm H II. The average distance of black holes in all phases is 1 kpc. Note that there is a rise in the number of

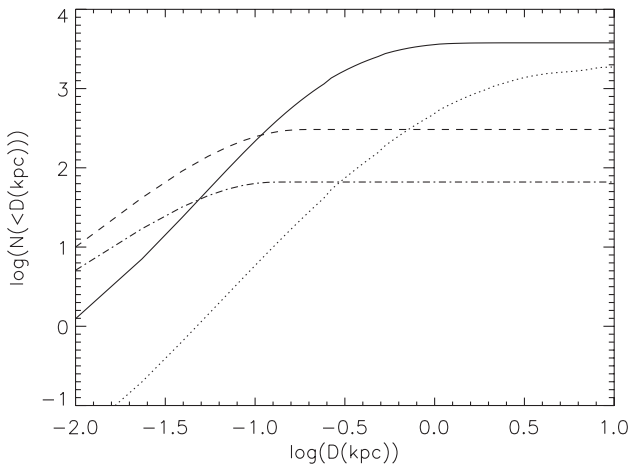

Figure 7. The total number of black hole sources with fluxes greater than $F = 10^{-15}\epsilon_{-5}\,{\rm erg\,cm^{-2}\,s^{-1}}$ and less distant than D. The solid line is for the CNM, the dotted line for the GMCs, the dashed line for the warm H I, and the dot-dashed line for the warm H II.

black holes in GMCs at the Galactic Centre (8 kpc away), since the surface density of molecular gas increases by a factor of $\sim$10 within 500 pc of the Galactic Centre. The sources in the gas clouds tend to be more distant, since it requires looking further in the Galaxy to find clouds, while the sources in the interstellar gas tend to be closer, since they are fainter due to lower accretion rates.

The sensitivity of the *ROSAT* All-Sky Survey (RASS) Bright Source Catalog is about $10^{-12}\,{\rm erg\,cm^{-2}\,s^{-1}}$ (Voges et al. 1999; we have converted count rate to flux assuming $\alpha = 1$), so at most $1N_9\epsilon_{-5}^{1.2}$ accreting black holes should have been detected by this survey, given the assumption of persistence. We can see immediately from Fig. 5 why it may have been difficult to detect isolated accreting neutron stars with the RASS, since we predict about one visible neutron star on the sky at this flux level, which will be reduced further by X-ray absorption. Danner (1998) has surveyed sources in molecular clouds within the RASS, finding no new isolated neutron-star candidates, and thus, we presume, no

isolated black hole candidates. For an X-ray observatory such as *EXIST*, which will reach sensitivities of $\sim 10^{-13}\,\mathrm{erg\,cm^{-2}\,s^{-1}}$ for one-year co-added data (Grindlay et al. 2000), about $\sim 50 N_9 \epsilon_{-5}^{1.2}$ sources may be detectable at hard X-ray energies as well. *EXIST* will have an angular resolution of about 2 arcmin and position sensitivity of ~ 30 arcsec, which should make identification feasible within molecular clouds.

The *Chandra* and *XMM-Newton* observatories have much better sensitivities $\sim 10^{-14}\,\mathrm{erg\,cm^{-2}\,s^{-1}}$ for a 10 kilosecond (ks) observation; however, both satellites have a much smaller field of view ($16 \times 16\,\mathrm{arcmin^2}$). The ChaMPlane survey (*Chandra* Multiwavelength Galactic Plane Survey; Wilkes et al. 2001) will cover about 1 square degree per year to a flux of $\sim 10^{-15}\,\mathrm{erg\,cm^{-2}\,s^{-1}}$ for the 1–10 keV band. This flux limit is deep enough that $\sim 6 \times 10^3 N_9 \epsilon_{-5}^{1.2}$ sources within the Galactic plane might be detectable (Fig. 5); however, the central 50 per cent are spread over an area of $4000\,\mathrm{deg^2}$ in the Galactic plane (Fig. 6). The *XMM-Newton* Serendipitous Survey will cover an area of the sky ~ 10 times larger than the *Chandra* Serendipitous Survey at similar sensitivity (Watson et al. 2001). Thus, these surveys may result in $\sim 10 N_9 \epsilon_{-5}^{1.2}$ detections per year.

One might expect that targeting molecular clouds may be advantageous for finding black holes. However, due to their proximity, the 23 clouds within 1 kpc have angular sizes of about 5°–20° (Dame et al. 1987), which will make them rather difficult to cover with the small field of view of *Chandra* or *XMM-Newton*. For instance, the single pointing in the ρ Ophiucus molecular cloud observed by Imanishi, Koyama & Tsuboi (2001) covers a volume $\sim 18\,\mathrm{pc^3}$ (assuming the cloud is spherical), so we expect only $\sim 3 \times 10^{-2} N_9$ black holes to reside within the observed volume. Observations pointed at molecular clouds will not improve these detection rates, but observations pointing toward the Galactic Centre should increase the number of detections significantly. Surveys targeted at the Galactic Centre (Baganoff et al. 2001) may find $1 N_9 \epsilon_{-5}^{1.2}$ per *Chandra* or *XMM-Newton* field.

6.2 Transient sources

The second assumption is that each of the sources are transient, driven by the hydrogen-ionization instability at radii in the accretion disc with $T \sim 5000$ K as in low-mass X-ray binaries. In this case, we assume that the sources undergo outbursts for several months with luminosities near the Eddington limit, while remaining faint for several decades. Chen, Shrader & Livio (1997, CSL in Table 1) have shown that soft X-ray transients tend to peak at $L_{\rm out} \sim 0.2 L_{\rm Edd}$ with an average duration (decay time-scale) of $t_{\rm o} \sim 20$ d and recurrence times varying from 2 to 60 yr for black holes. These are only the observed transients; transients with longer recurrence time-scales may not have had time to repeat. If we assume that each black hole accretes quiescently for a time $t_{\rm q}$, storing up mass in the accretion disc with a small fraction of gas accreting on to the black hole, and that all of this mass is then released in an outburst of duration $t_{\rm o}$, then

$$t_{\rm q} = 130\,\mathrm{yr}\,\frac{L_{\rm out}}{0.2 L_{\rm Edd}}\,\frac{t_{\rm o}}{20\,\mathrm{d}}\left(\frac{\epsilon_{\rm o}\dot{M}}{10^{14}\,\mathrm{g\,s^{-1}}}\right)^{-1}\frac{M}{9\,\mathrm{M_\odot}}, \qquad (14)$$

where $\epsilon_{\rm o}$ is the radiative efficiency of accretion during outburst. The outburst rate in the Milky Way is then

$$\dot{N}_{\rm out} = \int_{M_1}^{M_2} \mathrm{d}M \int_0^\infty \mathrm{d}\dot{M}\,\frac{\mathrm{d}^2 N}{\mathrm{d}M\,\mathrm{d}\dot{M}}\,t_q^{-1}. \qquad (15)$$

Assuming a 10 per cent efficiency during outburst, we find $\dot{N}_{\rm out} \sim 536 N_9\,\mathrm{yr^{-1}}$ for $\sigma_v = 40\,\mathrm{km\,s^{-1}}$. This is clearly inconsistent with observations, demonstrating that not all isolated black holes undergo transient outbursts if the assumptions of our calculation are correct. If only black holes accreting above $\dot{M} > 10^{15}\,\mathrm{g\,s^{-1}}$ undergo outbursts, consistent with the observed X-ray novae (van Paradijs 1996), then these numbers reduce to $50\,\mathrm{yr^{-1}}$, still large given that ~ 1 transient is detected each year, and generally they are found to have companions. We conclude that only a small fraction of isolated black holes might experience transience similar to X-ray novae. A different sort of instability due to magnetic suspension of accretion was proposed to lead to outbursts in the case of isolated accreting neutron stars (Treves, Colpi & Lipunov 1993); such events have not been detected.

6.3 Detecting microlensing candidates

Several long-duration microlensing events towards the bulge of the Milky Way have significant probabilities of being due to black hole lenses (Bennett et al. 2001; Mao et al. 2002). However, these events may also be due to more distant, lower mass lenses (Agol et al. 2002). One possible way to constrain the mass of these lenses is to look for X-rays from accretion. Fig. 8 shows the flux as a function of distance for MACHO 96-BLG-5, MACHO 98-BLG-6, and MACHO-99-BLG-22 (OGLE-1999-BUL-32) (Mao et al. 2002) for a number density of $1\,\mathrm{cm^{-3}}$ with the total velocity set to $\sqrt{3/2}$ times the observed sky velocity projected on to the lens plane (ignoring the unknown projected source velocity) and subtracted from the Galactic rotation velocity ($220\,\mathrm{km\,s^{-1}}$) and an X-ray efficiency of $\epsilon_{\rm ion} = 10^{-3}$. We note that if the sky velocity of the source is significant, then the inferred lens velocity will be different, typically smaller, and this will increase the luminosity. The flux scales as $F \propto \epsilon n D^{-4}$ for small distances, since the mass depends on the inverse of the distance and the flux decreases as the inverse of distance squared. Observing in the X-ray would be advantageous to avoid confusion with the background microlensed star. In the soft X-ray band, a 1–10 keV flux of $\sim 10^{-15}\,\mathrm{erg\,cm^{-2}\,s^{-1}}$ can be detected with a ~ 400 ks exposure with *Chandra* or ~ 200 ks with *XMM-Newton*. A detection of a black hole candidate at such a flux level will allow an upper limit on the distance of ~ 1–3 kpc to be placed, assuming that they accrete from the diffuse ISM with $n < n_{\rm max} = 1\,\mathrm{cm^{-3}}$ and assuming an X-ray efficiency less than

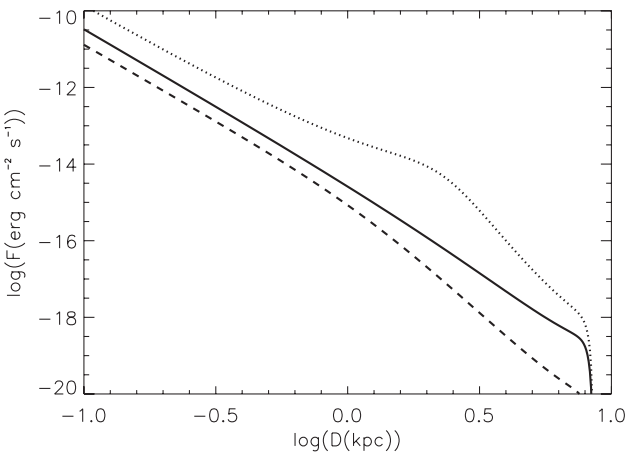

Figure 8. The flux as a function of distance for MACHO 96-BLG-5 (solid line), MACHO 98-BLG-6 (dashed line) and MACHO-99-BLG-22 (dotted line) for $\epsilon_{\rm ion} = 10^{-3}$.

$\epsilon_{\max} = 10^{-3}$. A decrease in efficiency will lead to a decrease in flux, and thus a decrease in the distance upper limit. An upper limit on distance converts into a lower limit on mass, since $M \propto D^{-1}$, which may confirm the black hole hypothesis. The mass lower limit is proportional to $M_{\min} \propto (\epsilon_{\max} n_{\max}/F)^{-1/4}$, a weak dependence on our assumed parameters. If enough X-rays are detected to measure the absorption column density towards the accreting MACHO can be measured, then the distance can be estimated from the roughly linear increase of column density in the direction of Baade's window (Arp 1965). A cloud or companion could increase the accretion rate, resulting in a higher luminosity, and hence a larger distance for the same flux; however, clouds occupy less than 5 per cent of the volume near the Galactic plane and can be searched for in H I at 21 cm or in CO absorption or emission (the MACHO fields are toward Baade's window, and are thus unlikely to contain a high molecular column density), while companions should be detectable with the *HST*.

7 CONCLUSIONS

We have estimated the number of isolated black holes that might be revealed by their X-ray emission from accretion of interstellar gas. We have improved upon previous calculations by taking into account the density distribution of the interstellar medium, as well as using the known properties of black hole X-ray binaries to constrain the phase-space and accretion efficiency of isolated accreting black holes. We conclude that persistent isolated black holes may be competitive with neutron stars in creating detectable X-ray flux if their efficiencies differ by $\epsilon_{\rm BH} \sim 10^{-4}\epsilon_{\rm NS}(N_{\rm BH}/N_{\rm NS})^{0.8}$, assuming that the Bondi–Hoyle accretion rate applies to both. The *ROSAT* survey did not have the sensitivity to detect either isolated accreting neutron stars or black holes; an all-sky survey with two orders of magnitude more sensitivity, $\sim 10^{-14}\,{\rm erg\,cm^{-2}\,s^{-1}\,dex^{-1}}$, may be able to detect $\sim 300 N_9 \epsilon_{-5}^{1.2}$ accreting black holes. The X-ray observatories *XMM-Newton* and *Chandra* may be able to detect this population with pointed observations; however, they suffer from having small fields of view. Despite this limitation, Galactic plane surveys being carried out with these telescopes may be able to detect tens per year for $\epsilon_{-5} = 1$. If the accreting sources with $\dot{M} > 10^{15}\,{\rm g\,s^{-1}}$ go through transient outbursts, then about 50 isolated black holes per year would be detectable as X-ray novae, so we reject this possibility since isolated X-ray novae have not been observed.

The greatest uncertainty in our predictions is the efficiency of black hole accretion, with which we have parameterised our results. Most of the detectable black holes should reside in interstellar clouds that have higher densities; however, this leads to the problem of confusion with other X-ray sources such as the coronae of massive stars. Some tests for whether an accreting object is a black hole are the following. (1) Is there high-energy emission? Accreting black holes tend to show spectra which have power laws extending up to $\sim 10^2\,{\rm keV}$ (Grove et al. 1998). (2) What is the nature of the variability? Accreting black holes show no pulsations, show only QPOs with $\nu < 1\,{\rm kHz}$, and show power spectra that cut off around 500 Hz (Sunyaev & Revnivtsev 2000). (3) What is the mass? Without a binary companion, the mass of an accreting object is difficult to measure; however, this might be achieved by carrying out astrometry of background stars to look for gravitational distortion by the accreting object (Paczyński 2001). (4) What do other parts of the spectra look like? Accreting black holes can produce relativistic radio jets (Mirabel & Rodríguez 1999), and photoionization of the surrounding gas might result in observable infrared lines (Maloney, Colgan & Hollenbach 1997).

There are several assumptions in our calculation that might affect the results. We have assumed that the accretion is time-steady; this may not be the case for higher accretion rates than we find for black holes accreting from the ISM (e.g. Grindlay 1978). If the black hole is moving slower than the sound speed at the accretion radius, then the preheated region outside the accretion radius may have a chance to expand into the ISM, reducing the number density, and thus reducing the accretion rate. If most black holes have companion stars, there may be an enhanced density of gas due to the wind from the companion. It may be that the bulk of black holes have a higher velocity dispersion than black hole X-ray binaries, which would reduce the accretion rates and reduce the number density of black holes in the plane. We have neglected mechanical feedback, which may occur if a jet or wind is developed. Recent work on non-radiating accretion flows indicates that strong winds can be formed which carry the bulk of the energy outwards as mechanical rather than radiative energy (Blandford & Begelman 1999; Igumenshchev, Abramowicz & Narayan 2000; Hawley, Balbus & Stone 2001; Abramowicz et al. 2002). These authors argue that the accretion rate scales as $\dot{M} \propto r$ into $r \sim 100 r_{\rm g}$. If the outer radius is taken as $r_{\rm A}$, then $\dot{M}(100 r_{\rm g}) \sim 100(v/c)^2 \dot{M}(r_{\rm A}) \sim 2 \times 10^{-5} v_{40}^{-2} \dot{M}(r_{\rm A})$. If the outer radius is taken to be the circularization radius, then $\dot{M}(100 r_{\rm g}) \sim 10^{-2}(M/9\,{\rm M_\odot})^{-2/3}[(v^2 + c_{\rm s}^2)^{1/2}/40\,{\rm km\,s^{-1}}]^{-10/3}$. Either of these circumstances will make black holes less visible, which in the formalism of this paper corresponds to a further reduction in the accretion efficiency. Magnetic fields will probably play an important role, as they are amplified by flux-freezing, possibly heating the gas to virial temperatures (Igumenshchev & Narayan 2002), and can transport angular momentum via the magneto-rotational instability once the circularization radius is reached, modifying the dynamics of the accretion flow, possibly extracting spin energy from the black hole (Armitage & Natarajan 1999). We have not explored the dependence of the efficiency on other parameters, which may result, for example, from changes in the gas density and angular momentum as a function of the accretion rate, so our extrapolation from estimated efficiencies of black hole X-ray binaries may be too optimistic. The validity of these assumptions can be tested with 3D radiation MHD simulations of a black hole accreting from an inhomogeneous medium, a daunting numerical problem.

It is possible that a population of intermediate-mass black holes (IMBHs) exist with larger masses around $250\,{\rm M_\odot}$, the remnants of the first generation of star formation (Madau & Rees 2001). The larger masses of these objects would result in yet larger accretion rates and luminosities by a factor of $\sim 10^3$, if they are distributed with same phase-space distribution as 9-$\rm M_\odot$ black holes. If we assume that $\sim 10^6$ IMBHs reside in the disc of our Galaxy, then we find that the number of detectable objects at high fluxes may be comparable to 9-$\rm M_\odot$ black holes accreting at the same efficiency (Fig. 5). However, if these objects reside in the halo or bulge of the Galaxy, the number detectable will be decreased significantly.

ACKNOWLEDGMENTS

We thank D. Bennett, L. Bildsten, O. Blaes, R. Blandford, J. Carpenter, D. Chernoff, G. Dubus, A. Esin, C. Fryer, J. Grindlay, T. Kallman, L. Koopmans, J. Krolik, Y. Lithwick, A. Melatos, S. Phinney, M. Rees, R. Rutledge, N. Scoville and K. Sheth for useful conversations and ideas which greatly improved this work.

This work was supported in part by NSF AST-0096023, NASA NAG5-8506, and DoE DE-FG03-92-ER40701. Support for the work done by EA was provided by the National Aeronautics and Space Administration through Chandra Postdoctoral Fellowship Award Number PF0-10013 issued by the Chandra X-ray Observatory Center, which is operated by the Smithsonian Astrophysical Observatory for and on behalf of the National Aeronautics Space Administration under contract NAS8-39073.

REFERENCES

Abramowicz M. A., Igumenshchev I. V., Quataert E., Narayan R., 2002, ApJ, 565, 1101
Agol E., Kamionkowski M., Koopmans L. V. E., Blandford R. D., 2002, ApJ, in press (astro-ph/0203257)
Armitage P. J., Natarajan P., 1999, ApJ, 523, 7
Armstrong J. W., Rickett B. J., Spangler S. R., 1995, ApJ, 443, 209
Arp H., 1965, ApJ, 141, 43
Baganoff F. K. et al., 2001, Nat, 413, 45
Bailyn C. D., Jain R. K., Coppi P., Orosz J. A., 1998, ApJ, 499, 367
Bennett D. P. et al., 2001, pre-print (astro-ph/0109467)
Berkhuijsen E. M., 1999, in Ostrowski M., Schlickeiser R., eds, Plasma Turbulence and Energetic Particles in Astrophysics. Kraków
Bildsten L., Rutledge R. E., 2000, ApJ, 541, 908
Blaes O. M., Madau P., 1993, ApJ, 403, 690
Blaes O., Warren O., Madau P., 1995, ApJ, 454, 370
Bland-Hawthorn J., Reynolds R., 2000, Encyclopedia of Astronomy & Astrophysics. MacMillan and Institute of Physics Publishing
Blandford R. D., Begelman M. C., 1999, MNRAS, 303, L1
Bondi H., Hoyle F., 1944, MNRAS, 104, 273
Brandt W. N., Podsiadlowski Ph., Sigurdsson S., 1995, MNRAS, 277, L35
Campana S., Pardi M. C., 1993, A&A, 277, 477
Carr B. J., 1979, MNRAS, 189, 123
Chen W., Shrader C. R., Livio M., 1997, ApJ, 491, 312 (CSL)
Clemens D. P., Sanders D. B., Scoville N. Z., 1988, ApJ, 327, 139
Colpi M., Turolla R., Zane S., Treves A., 1998, ApJ, 501, 252
Cordes J. M., Chernoff D. F., 1998, ApJ, 505, 315
Dame T. M. et al., 1987, ApJ, 322, 706
Danner R., 1998, A&AS, 128, 331
Dickey J. M., Garwood R. W., 1989, ApJ, 341, 201
Dubinski J., Narayan R., Phillips T. G., 1995, ApJ, 448, 226
Fender R., 2001, MNRAS, 322, 31
Fryer C. L., Kalogera V., 2001, ApJ, 554, 548
Fujita Y., Inoue S., Nakamura T., Manmoto T., Nakamura K. E., 1998, ApJ, 495, L85
Garcia M. R., McClintock J. E., Narayan R., Callanan P., Murray S. S., 2001, ApJ, 553, L47
Grindlay J., 1978, ApJ, 221, 234
Grindlay J. et al., 2000, in McConnell M. L., Ryan J. M., eds, Am. Inst. Phys. Conf. Proc. Vol. 510, The Fifth Compton Symposium. AIP, New York, p. 784
Grindlay J. et al., 2001, in Ritz S., Geherels N., Schrader C. R., eds, Am. Inst. Phys. Conf. Proc. Vol. 587, GAMMA 2001. Gamma-Ray Astrophysics 2001. AIP, New York, p. 899
Grove J. E., Johnson W. N., Kroeger R. A., McNaron-Brown K., Skibo J. G., Phlips B. F., 1998, ApJ, 500, 899
Hansen B. M. S., Phinney E. S., 1997, MNRAS, 291, 569
Hawley J. F., Balbus S. A., Stone J. M., 2001, ApJ, 554, L49
Heckler A. F., Kolb E. W., 1996, ApJ, 472, L85
Iben I., Jr, Tutukov A. V., Yungelson L. R., 1995, ApJS, 100, 233
Igumenshchev I. V., Abramowicz M. A., Narayan R., 2000, ApJ, 537, L27
Igumenshchev I. V., Narayan R., 2002, ApJ, 566, 137
Imanishi K., Koyama K., Tsuboi Y., 2001, ApJ, 557, 747
Ipser J. R., Price R. H., 1977, ApJ, 216, 578
Ipser J. R., Price R. H., 1982, ApJ, 255, 654
Ipser J. R., Price R. H., 1983, ApJ, 267, 371
Kong A. K. H., McClintock J. E., Garcia M. R., Murray S. S., Barret D., 2002, ApJ, 570, 277
Koyama K., Maeda Y., Sonobe T., Takeshima T., Tanaka Y., Yamauchi S., 1996, PASJ, 48, 249
Larson R. B., 1981, MNRAS, 194, 809
Lasota J. P., 2000, A&A, 360, 575
Lasota J. P., 2001, New Astron. Rev., 45, 449
Lazarian A., Pogosyan D., 2000, ApJ, 537, 720
Livio M., Xu C., Frank J., 1998, ApJ, 492, 298
Loewenstein M., Mushotzky R. F., Angelini L., Arnaud K. A., Quataert E., 2001, ApJ, 555, L21
Madau P., Rees M. J., 2001, ApJ, 551, L27
Maloney P. R., Colgan S. W. J., Hollenbach D. J., 1997, ApJ, 482, L41
Mao S. et al., 2002, MNRAS, 329, 349
McDowell J., 1985, MNRAS, 217, 77
Mirabel I. F., Rodríguez L. F., 1999, ARA&A, 37, 409
Mirabel I. F., Dhawan V., Mignani R. P., Rodrigues I., Guglielmetti F., 2001, Nat, 413, 139
Morrison R., McCammon D., 1983, ApJ, 270, 119
Narayan R., Yi I., 1994, ApJ, 428, L13
Narayan R., Garcia M. R., McClintock J. E., 2002, in Gurzadyan V. G., Jantzen R. T., Ruffini R., eds, Proc. 9th Marcel Grossman Meeting on General Relativity. World Scientific, Singapore, p. 396
Nelemans G., Tauris T. M., van den Heuvel E. P. J., 1999, A&A, 352, L87
Orosz J. A., Jain Raj K., Bailyn C. D., McClintock J. E., Remillard R. A., 1998, ApJ, 499, 375
Ostriker J. P., Rees M. J., Silk J., 1970, Astrophys. Lett., 6, 179
Ostriker J. P., McCray R., Weaver R., Yahil A., 1976, ApJ, 208, L61
Paczyński B., 2001, astro-ph/0107443
Popov S. B., Prokhorov M. E., 1998, A&A, 331, 535
Ruffert M., 1999, A&A, 346, 861
Rutledge R. E., Bildsten L., Brown E. F., Pavlov G. G., Zavlin V. E., 2001a, ApJ, 551, 921
Rutledge R. E., Bildsten L., Brown E. F., Pavlov G. G., Zavlin V. E., 2001b, ApJ, 559, 1054
Samland M., 1998, ApJ, 496, 155
Schwope A. D., Hasinger G., Schwarz R., Haberl F., Schmidt M., 1999, A&A, 341, L51
Scoville N. Z., Sanders D. B., 1987, in Hollenbach D. J., Thronson H. A., eds, Interstellar Processes. Reidel, Dordrecht, p. 21
Shapiro S. L., Lightman A. P., 1976, ApJ, 204, 555
Shapiro S. L., Teukolsky S. A., 1983, Black Holes, White Dwarfs and Neutron Stars. Wiley-Interscience, New York
Shvartsman V. F., 1971, Sov. Astron. AJ, 14, 662
Stocke J. T., Wang Q. D., Perlman E. S., Donahue M. E., Schachter J. F., 1995, AJ, 109, 1199
Sunyaev R., Revnivtsev M., 2000, A&A, 358, 617
Thorsett S. E., Chakrabarty D., 1999, ApJ, 512, 288
Treves A., Colpi, 1991, A&A, 241, 107
Treves A., Colpi M., Lipunov V. M., 1993, A&A, 269, 319
Treves A., Turolla R., Zane S., Colpi M., 2000, PASP, 112, 297
van den Heuvel E. P. J., 1992, Environment Observation and Climate Modeling Through International Space Projects. ESA Publications Division, Noordwijk
van Paradijs J., 1996, ApJ, 464, L139
van Paradijs J., White N. E., 1995, ApJ, 447, L33
Voges W. et al., 1999, A&A, 349, 389
Walter F. M., Wolk S. J., Neuhauser R., 1996, Nat, 379, 233
Wang J. C. L., 1997, ApJ, 486, L119
Watson M. G. et al., 2001, A&A, 365, L51
White N. E., van Paradijs J., 1996, ApJ, 473, L25 (WvP)
Wilkes B. J. et al., 2001, in Clowes R., Adamson A., Bromage G., eds, ASP Conf. Ser. Vol. 232, The New Era of Wide Field Astronomy. Astron. Soc. Pac., San Francisco, p. 47
Wilson C. D., Done C., 2001, MNRAS, 325, 167

This paper has been typeset from a TEX/LATEX file prepared by the author.